Proc. 10th Int. Workshop on Neutrino-Nucleus Interactions in Few-GeV Region (NuInt15)
JPS Conf. Proc. **12**, 010016 (2016)
https://doi.org/10.7566/JPSCP.12.010016

Muon Neutrino CCQE at MINERvA

M. Betancourt

Fermi National Accelerator Laboratory, Batavia, Illinois 60510, USA

E-mail: betan009@fnal.gov

(Received January 13 2016)

A precise understanding of quasi-elastic interactions is crucial to measure neutrino oscillations. The MINERvA experiment is currently working on different analyses of muon neutrino charged current quasi-elastic interactions. We present updates to the previous quasi-elastic measurement, using a new flux, and we present the status of several analyses in progress; including double differential cross sections, a study of final state interactions using a sample with muon and a proton and the status of the CCQE analysis in the medium energy neutrino beam.

1. Introduction

Accurate neutrino cross section measurements and studies of nuclear effects are required for precise measurements of neutrino oscillation parameters, CP-violation in the lepton sector, and the orientation of the neutrino mass hierarchy. Charged-Current Quasi-Elastic (CCQE) scattering is a very important channel for neutrino oscillation experiments. Experiments such as T2K use CCQE interactions as the main channel for appearance and disappearance measurements [1].

The MINERνA experiment is designed to perform precision measurements of neutrino-nucleus scattering using neutrinos and antineutrinos. We present update measurements of differential cross sections of CCQE scattering for neutrinos and antineutrinos, as well as the status of analyses in progress.

The MINERνA experiment uses neutrinos from the main Injector (NuMI) beam at Fermi National Accelerator Laboratory [2]. The neutrinos are generated by focusing 120 GeV protons from the main injector onto a graphite target. This interaction produces mesons (pions and kaons), which are focused by two magnetic focusing horns located downstream of the target. The mesons decay and produce neutrinos. Changing the horn current polarity produces either a neutrino or an antineutrino beam. The analyses use all the data collected using the low energy neutrino beam ($E \sim 3.5GeV$) and the recent data collected using a medium energy neutrino beam ($E \sim 6GeV$) .

The MINERνA detector is comprised of 120 hexagonal modules perpendicular to the z-axis. MINERνA is segmented transversely into: the inner detector, with planes of solid scintillator strips mixed with nuclear targets; a region of pure scintillator strips; downstream electromagnetic calorimeter and hadronic calorimeters; and an outer detector composed of a frame of steel with embedded scintillator, which also serves as the supporting structure. The scintillator strips in adjacent planes are offset by 60° from each other, which enables a three-dimensional track reconstruction [3]. The MINOS near detector is two meters downstream of the MINERνA detector and serves as a magnetized muon spectrometer [4].

2. Updates to previous CCQE measurements

Differential cross section measurements have been reported by MINERvA and compared with different model predictions [5, 6]. We present updates to these measurements. Several improvements

have been made to the neutrino flux prediction, including updates to the beamline geometry and constraints the simulation with hadron production data [7]. Figures 1 and 2 show comparisons of the measured differential cross sections with respect to Q^2 and different theoretical models for neutrinos and antineutrinos. The top left distribution is the old measurement and the top right is the updated measurement for comparison, since the new flux is lower the differential cross section is increased. The bottom distribution is the ratio of the updated measurement to GENIE simulation. We use the GENIE and NuWro simulations [8], where GENIE uses the Relativistic Fermi Gas model (RFG) with an axial mass of $M_A = 0.99 GeV/c^2$ and NuWro uses RFG model and different M_A values. In addition, NuWro includes the Spectral Function (SF) model, which is a more realistic model of the nucleon momentum, and a transverse enhancement model (TEM) tuned to electron-nucleon scattering data to account for correlated nucleon target [9].

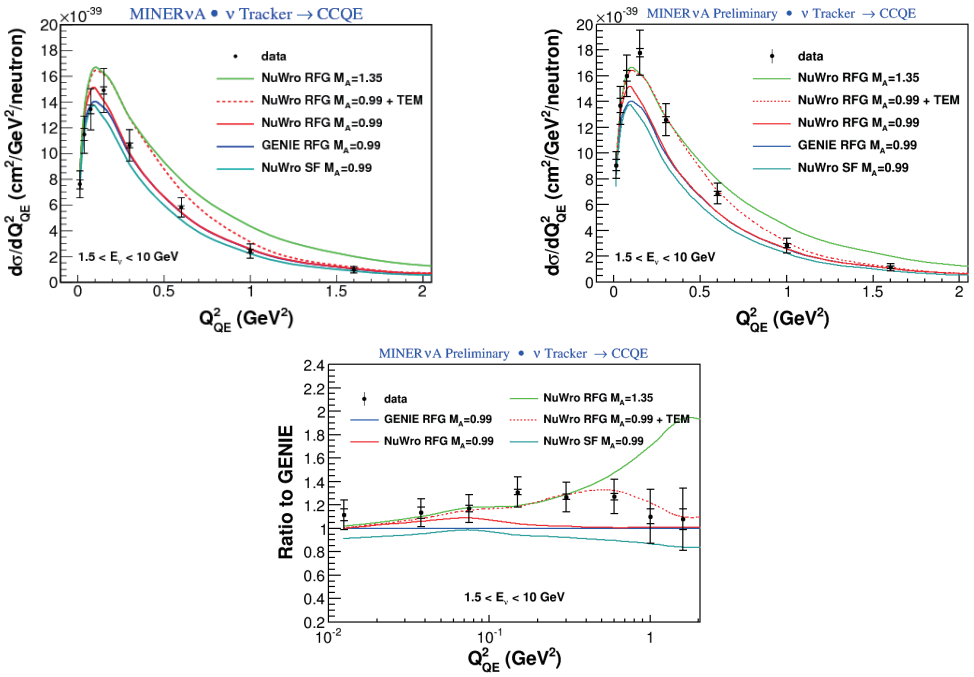

Fig. 1. Differential cross section compared with GENIE and NuWro simulations for the neutrinos analysis (top), left is the old differential cross section measurement [5] and right is the updated measurement. Ratio of the updated differential cross section to GENIE simulation for neutrinos (bottom).

The data is consistent with the TEM with $M_A = 0.99 GeV/c^2$. Table I and Table II shows the comparison of the $\chi^2/d.o.f.$ for the published and updated measurements for neutrinos and antineutrinos. For both measurements, the best agreement is with NuWro (TEM, $M_A = 0.99 GeV/c^2$) prediction.

Table I. Comparison of the $\chi^2/d.o.f.$ between the [5] and the updated measurement for the neutrinos

Simulation	$\chi^2/d.o.f.$([5] measurement)	$\chi^2/d.o.f.$(Updated measurement)
NuWro($M_A = 0.99$)	3.5	5.25
NuWro($M_A = 1.35$)	3.7	6.4
NuWro($M_A = 0.99$)TEM	2.4	2.7
NuWro($M_A = 0.99$)SLF	2.8	5.6

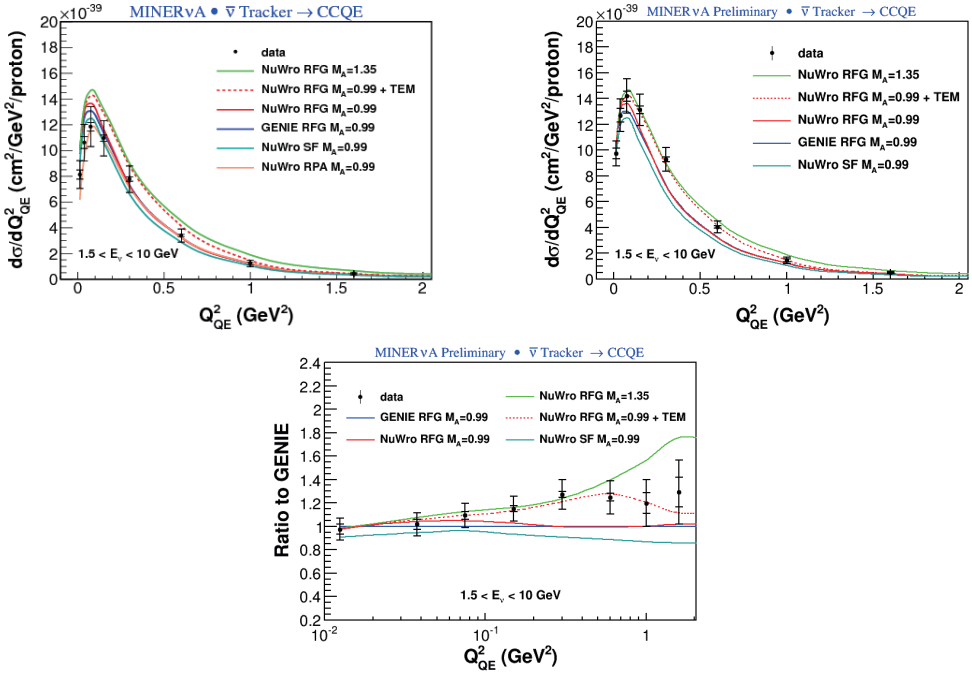

Fig. 2. Differential cross section compared with GENIE and NuWro simulations for the antineutrinos analysis (top), left is the old differential cross section measurement [6] and right is the updated measurement. Ratio of the updated differential cross section to GENIE simulation for antineutrinos (bottom).

Table II. Comparison of the $\chi^2/d.o.f.$ between the [6] and the updated measurement for the antineutrinos

Simulation	$\chi^2/d.o.f.$([6] measurement)	$\chi^2/d.o.f.$(Updated measurement)
NuWro(M_A = 0.99)	2.6	3.1
NuWro(M_A = 1.35)	2.9	3.5
NuWro(M_A = 0.99)TEM	1.06	0.95
NuWro(M_A = 0.99)SLF	2.8	3.65

The CCQE analyses of neutrinos and antineutrinos previously reported [5], [6] used the signal definition as an event in which the primary interaction is quasi-elastic (regardless of the final state particles) and the incoming neutrino energy is required between 1.5 and 10 GeV. The CCQE analyses in progress use a new definition for the signal, quasi-elastic like, in which there are not pions in the final sate. The next sections provide the selection details for each analysis.

3. Study of Final State Interactions (FSI)

Final state interactions are very important for neutrino scattering, they change the topology of the initial interactions and the kinematic of the event, what we measure in our detectors is different from what the initial neutrino interaction produces. The effect produced by final state interactions is harder to measure in neutrino scattering because we do not know the incoming neutrino energy. We select a CCQE like sample with a muon and proton that allows us to do further studies of final state interactions.

We study the CCQE like scattering for neutrinos using muon and proton kinematics. The selection uses the following criteria: (1)Events with two or more tracks, where one track is the muon and

the other tracks are protons, (2) At least one proton with momentum greater than $450 MeV/c$. This requirement comes from the threshold of the proton reconstruction. (3) Identified protons, require the hadrons to look like protons using the dE/dx, (4) Inelastic background with untracked pion is removed by cutting on energy, E_{extra}, that is not linked to a track and is located outside of a 10 cm sphere centered at the vertex, (5) Pions of kinetic energy below 100 MeV are removed using Michel electrons. The definition for the signal is CCQE like events with no pions in the final state.

We study different regions of coplanarity angle, which is the angle between the ν-muon and ν-proton planes:

$$\phi = cos^{-1}\left(\frac{(\vec{p}_\nu \times \vec{p}_\mu).(\vec{p}_\nu \times \vec{p}_p)}{|\vec{p}_\nu \times \vec{p}_\mu|.|\vec{p}_\nu \times \vec{p}_p|}\right). \tag{1}$$

Figure 3 shows the coplanarity angle, where dots show the data, the red curve is the simulation with FSI, the blue curve is the simulation without FSI and the background prediction is shown. The background prediction has been tuned to the data. Four sidebands are used to extract normalization constants for two separate processes; resonant and "DIS plus other", where other includes a small component of neutral current and $\bar{\nu}_\mu$. The normalization constant are determined from linear fit that matches the simulated background to data [10,11]. The background is dominated by resonance events. For CCQE scattering off a free neutron at rest, $\varphi = 180$. The detector resolution on φ is 3.8 degrees, so the width shown on the distributions in Figure 3 is due to Fermi motion, inelastic scattering, and FSI effects. The comparison shows that GENIE with FSI describes the data better than GENIE without FSI [10]. We can see this distribution is sensitive to final state interactions.

To study further the final state interactions we select three regions of the coplanarity angle; from 0 to 110 degrees, from 110 to 160 degrees and from 160 to 180 degrees. The different regions have different populations of events. The region from 0 to 110 and from 110 to 160 are mostly dominated by background, while the region from 160 to 180 is mostly CCQE like events.

To study the FSI we define the difference of the measured proton momentum and expected proton momentum

$$\Delta P = P_{measured} - P_{Expected}, \tag{2}$$

where $P_{Expected}(E_\nu, E_\mu)$ is obtained from the angle and energy of the muon. Only the leading proton is considered in equation 2 and in the distributions. Figure 4 shows the distributions for the different coplanarity angles, the plot on the left is from 0 to 110 degrees, the middle plot is from 110 to 160 degrees and the right distribution is from 160 to 180 degrees. The background on these distributions is dominated by resonance interactions. The red is the simulation with FSI, the blue is the simulation without FSI, the grey distribution is the background for FSI. This background has been tuned to the simulation with FSI and the simulation without FSI has not been tuned. The distributions are normalized to a common normalization for all φ. The comparison shows that GENIE with FSI describes the data better than GENIE without FSI. These set of distributions are sensitive to final state interactions.

In addition, we plot the difference between the neutrino energy predictions in figure 5. The difference is computed using the neutrino energy from the proton and muon energies,

$$E_\nu = E_\mu + T_p + BE, \tag{3}$$

and the neutrino energy computed from the QE hypothesis using

$$E_{QE} = \frac{m_n^2 - (m_p - E_b)^2 - m_\mu^2 + 2(m_p - E_b)E_\mu}{2(m_p - E_b - E_\mu + p_\mu \cos\theta_\mu)}, \tag{4}$$

where BE is the binding energy (34 MeV), m_p is the mass of proton, m_n is the mass of the neutron, E_μ and θ_μ are the energy, and angle of the muon. Three sets of distributions are shown in figure 5, left distribution is for events with coplanarity angle between 0 to 110 degrees, middle is for events with

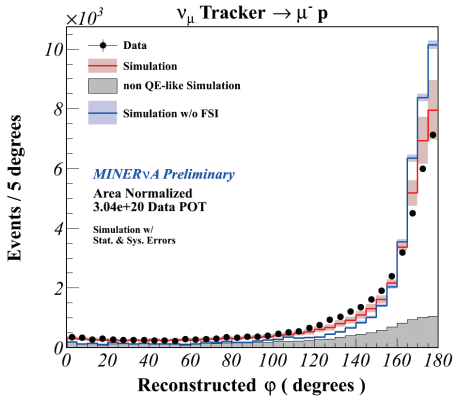

Fig. 3. Angle between the *ν*-muon and *ν*-proton planes for data and GENIE simulations, where the red prediction includes FSI and the blue does not. The total predictions have been normalized to the data [10].

coplanarity angle between 110 to 160 degrees and right distribution is for events with coplanarity angle between 160 to 180 degrees. The comparison, again shows that GENIE with FSI describes the data better than GENIE without FSI.

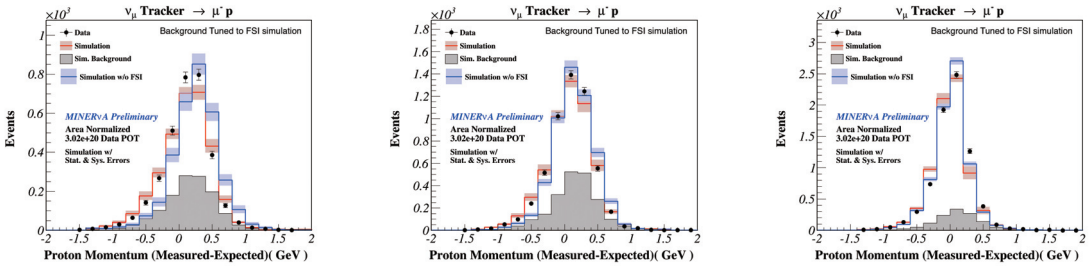

Fig. 4. Proton momentum measured minus the expected for three different regions of the coplanarity angle, where expected is the momentum calculated from the muon kinematics. Distribution for 0 to 110 degrees (left), distribution for 110 to 160 degrees (middle) and distribution for 160 to 180 degrees (right).

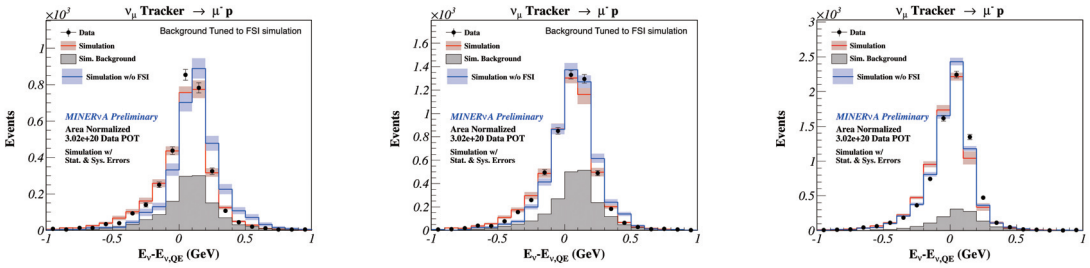

Fig. 5. Neutrino energy predicted from the proton and muon minus the neutrino energy from the QE hypothesis. Distribution for 0 to 110 degrees (left), distribution for 110 to 160 degrees (middle) and distribution for 160 to 180 degrees (right).

4. Double Differential Cross Section

A double differential cross section analyses is in progress. The muon longitudinal P_{II} and the transverse momentum P_T are the measurable quantities:

$$\frac{d^2\sigma}{dP_T dP_{II}} \tag{5}$$

P_{II} and P_T are less model dependent than four momentum transfer, Q^2. In addition, P_{II} is correlated with the neutrino energy and P_T is correlated with Q^2. The double differential cross section will help discriminate between models. Two analyses are underway to constraint the CCQE cross sections; for neutrinos and antineutrinos. We present the status of the analysis selection for both modes.

4.1 Selected Events in Neutrino

We study CCQE scattering for neutrinos using the muon kinematics. The selection uses the following criteria: (1) Selected muon, (2) If second track found, it is require to be consistent with a proton, (3) Removed pions with a Michel electron veto, (4) Require the Q^2 dependent recoil energy cut. The recoil energy is the energy outside of the vertex region [5, 6]. The definition is CCQE-like, any number of nucleons, but no pions. Figure 6 shows the event distributions versus transverse muon momentum P_T, for different bins longitudinal muon momentum, P_{II}. We have a very high statistic sample for neutrinos with about 80,000 selected events. Red is GENIE simulation and the grey distribution is the predicted background. The uncertainties are from reconstruction and the interaction model, including the CCQE uncertainty. The distributions show good data simulation agreement.

4.2 Selected Events in Antineutrino Beam

The analysis for the antineutrino sample uses the kinematics of the muon and we define the same quantities described for the neutrino analysis. The preliminary selection uses the following criteria: (1) Selected muon, (2) Require only a muon track, and one isolated energy showers, (3) Require the Q^2 dependent recoil energy cut. The signal definition for the final analysis will be CCQE-like. This preliminary selection does not include the $CC0\pi$ events that are not CCQE, because we have a low acceptance for the $CC0\pi$ events. The recoil energy cut removes events with a second neutron. Final selection is in preparation. Figure 7 shows the events distributions versus longitudinal muon momentum, P_T, for different bins of transverse muon momentum, P_{II}. This preliminary selection contain about 16000 selected events. Red is GENIE simulation and the grey distribution is the predicted background. The uncertainties are from reconstruction and the interaction model, including the CCQE uncertainty. The distributions shows good data simulation agreement.

Both samples for neutrinos and antineutrinos have high statistics. The double differential cross

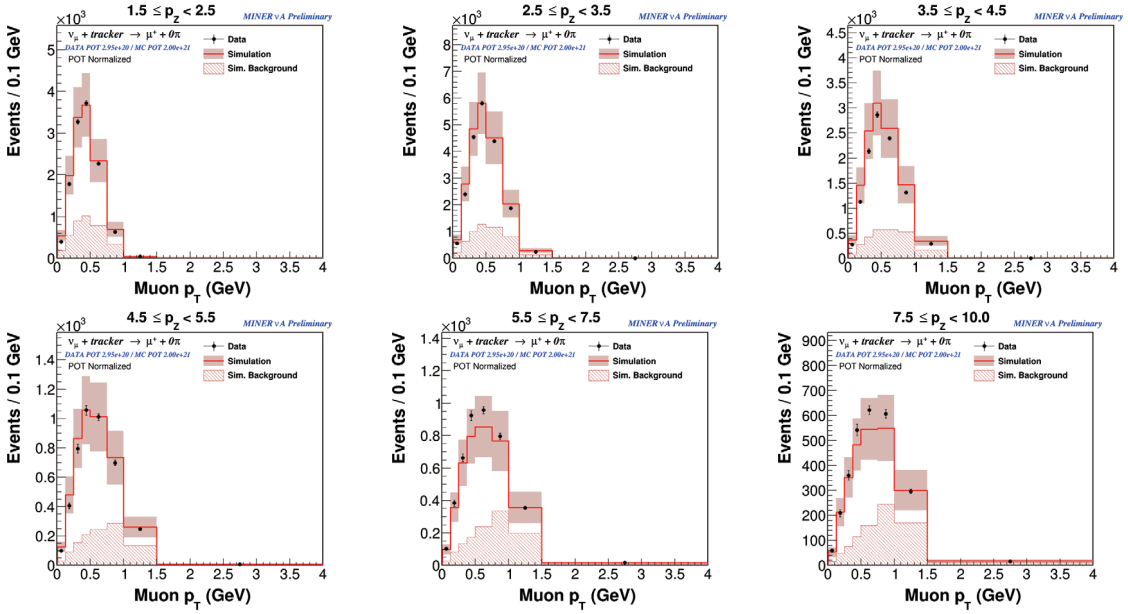

Fig. 6. Data and GENIE simulation event distributions versus transverse muon momentum in bins of longitudinal muon momentum for neutrinos. Dash curve is the predicted background.

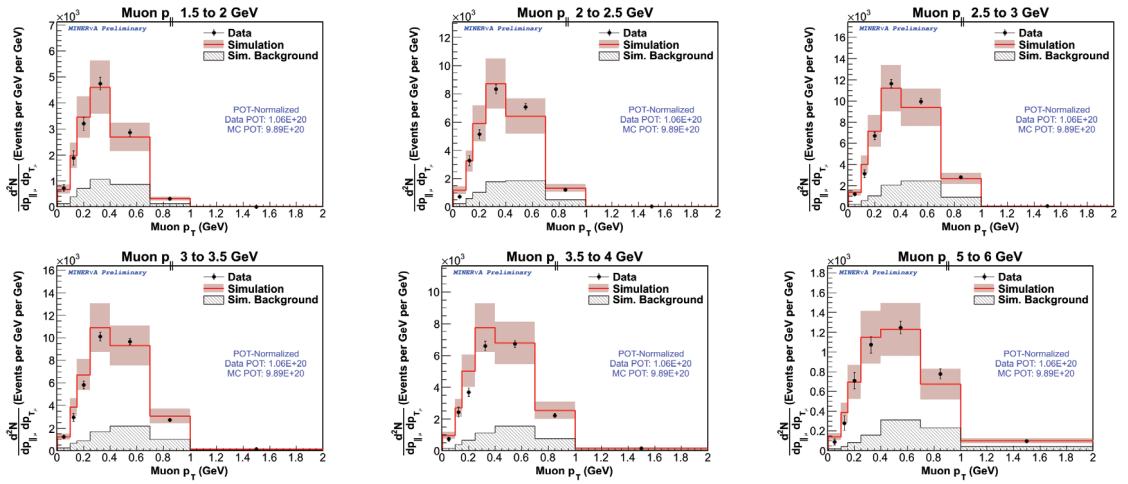

Fig. 7. Data and GENIE simulation event distributions versus transverse muon momentum in bins of longitudinal muon momentum for antineutrinos. Gray curve is the predicted background.

section measurements should give additional power to distinguish between models.

5. CCQE in Medium Energy Beam

MINERVA is collecting data with the medium energy beam, we have collected $6E20POT$. We are analyzing these data, a preliminary selection is shown in Figure 8 for the reconstructed muon energy and the reconstructed muon angle. We require a muon in the event and the muon track in MINERvA extending into MINOS. Distributions show the data in black, the GENIE prediction and the untuned background prediction. For small data set of the medium energy ($8.8E20POT$) we have

about 117000 selected events. A more sophisticate selection is underway, which uses the Michel veto and proton selection.

The data set at medium energy will provide constraint at high Q^2, where the statistic was low at the low energy beam.

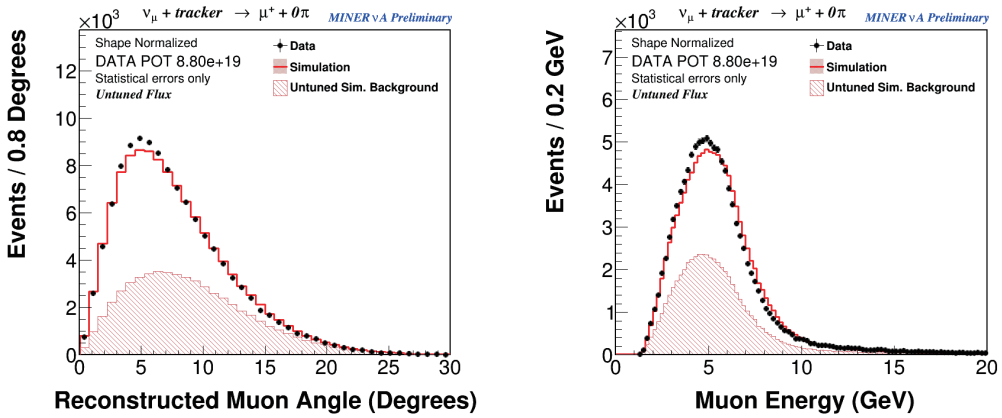

Fig. 8. Reconstructed muon angle (left) and reconstructed muon energy (right) for events with a muon track in MINERvA extending into MINOS experiment. The backgrounds are untuned and only statistics errors are shown in the distributions. The GENIE simulation has been normalized to the number of events in data.

6. Summary

Flux updated ν_μ and $\bar{\nu}_\mu$ CCQE differential cross sections are reported. The measured differential cross sections for neutrinos and antineutrinos, $d\sigma/dQ^2$, disfavor a simple Relativistic Fermi Gas model and agree with a transverse enhancement model with $M_A = 0.99 GeV/c^2$. MINERvA has a dedicated program to study CCQE scattering. Further analyses are underway to constrain different cross sections and understand final state interactions, such as double differential cross sections for neutrinos and antineutrinos and the study of final state interactions using the low energy beam from NuMI; and cross sections using the medium energy beam from NuMI.

References

[1] K. Abe *et al.* [T2K Collaboration], Phys. Rev. Lett. **107**, 041801 (2011); Phys. Rev. Lett. **112**, 068103 (2013).
[2] K. Anderson, B. Bernstein, D. Boehnlein, K. R. Bourkland, S. Childress, N. Grossman, J. Hylen and C. James *et al.*, FERMILAB-DESIGN-1998-01.
[3] L. Aliaga et al., Nucl. Instrum. Meth. **A743**, 130 (2014).
[4] D. G. Michael *et al.*, Nucl. Instrum. Meth., **A596**, 190 (2008).
[5] G. A. Fiorentini *et al.*, Phys. Rev. Lett. **111**, 022502 (2013).
[6] L. Fields *et al.*, Phys. Rev. Lett. **111**, 022501 (2013).
[7] L. Aliaga, FNAL JTEP, 17 December 2015.
[8] C. Andreopoulos, A. Bell, D. Bhattacharya, F. Cavanna, J. Dobson, S. Dytman, H. Gallagher and P. Guzowski *et al.*, Nucl. Instrum. Meth. A **614** 87 (2010). T. Golan, C. Juszczak, and J. Sobczyk, Phys. Rev. C **85** (2012). R. Smith and E. Moniz, Nucl. Phys. B **43**, 605 (1972).
[9] O. Benhar, A. Fabrocini, S. Fantoni, and I. Sick, Nucl.Phys. A **579**, 493 (1994). A. Bodek, H. Budd, and M. Christy, Eur.Phys.J. C**71**, 1726 (2011).
[10] T. Walton *et al.*, Phys. Rev. D **91**, (2015).
[11] T. Walton FERMILAB-THESIS-2014-11, Hampton University, (2014).